

# Simulation of Solute Transport in a Finite Aquatic Ecosystem Using the Two-Dimensional Advection-Dispersion Equation in Cylindrical Coordinates: Analysis of the Impact of Emergent and Rigid Vegetation

## ABSTRACT

*Aquatic porous media experience the intrusion of pollutants from natural or anthropogenic sources, affecting the health of aquatic ecosystems. The retention and diffusion of pollutants strongly depend on parameters such as vegetation volumetric fraction ( $\phi$ ), porosity, and medium density. This study numerically solves the advection-dispersion equation in cylindrical coordinates using finite difference methods to evaluate pollutant concentration profiles in an initially contaminated aquatic porous medium, where flow velocity and dispersion coefficient vary with the vegetation fraction. The results reveal a marked sensitivity of concentration profiles to an increase in vegetation fraction, which reduces pollutant diffusion, while higher porosity promotes their dispersion. Furthermore, zones of **high-medium** density accumulate more pollutants, increasing local concentrations. These interactions influence aquatic ecosystems, with elevated concentrations potentially disrupting flora and fauna. This study highlights the importance of considering these parameters to develop effective strategies for the management and preservation of aquatic environments.*

**Keywords:** **aquatic** environments, pollutants, cylindrical coordinates, flora, fauna.

## 1. INTRODUCTION:

Nowadays, humanity faces major challenges, among which health and food security stand out as crucial issues. To address these, humanity turns to the chemical and pharmaceutical industries [1]. On one hand, these industries improve agricultural yields through fertilizers and pesticides, and on the other hand, they develop medicines to combat diseases. However, despite their benefits, these products pose significant environmental problems, notably the degradation of aquatic biodiversity and groundwater pollution [1-2]. Consequently, the transport of pollutants in porous and aquatic underground environments has drawn the **scientific community's attention**, with the objectives of better controlling these processes and implementing appropriate measures to limit environmental impacts.

The transport of contaminants in porous aquatic environments is strongly influenced by emergent vegetation, which reduces flow velocity and limits pollutant propagation [3]. By

31 increasing turbulence, vegetation also promotes solute mixing, contributing to the  
32 protection of aquatic habitats and ecosystem health [3].

33 To describe the transport of dissolved contaminants in these environments, the advection-  
34 dispersion model is commonly used, with adjustments that vary depending on the types  
35 of contaminants [4,5,6]. The advection-dispersion equation in cylindrical coordinates  
36 offers specific advantages for modeling pollutants in porous environments compared to  
37 Cartesian coordinates [7]. In cylindrical coordinates, its better models' radial flows and  
38 diffusion configurations are dependent on the radius, which is useful for point or variable  
39 pollution sources [7,8,9]. This framework simplifies the analysis of concentrations by  
40 incorporating adapted boundary conditions, such as unstable flow rates and radial  
41 geometry, offering optimized solutions for heterogeneous or homogeneous aquifers.

42 Several researchers have focused on this area of research. For instance, [7] studied the  
43 effect of an exponentially decreasing flow velocity over time, associated with solute  
44 injection radii, on concentration profiles in a finite cylindrical domain by numerically solving  
45 the advection-dispersion equation in cylindrical coordinates. [3] used a model based on  
46 the advection-dispersion equation in Cartesian coordinates to describe how emergent and  
47 rigid vegetation influences solute and particle transport in aquatic ecosystems. [10]  
48 developed a risk assessment model for accidental spills of silver nanoparticles (AgNPs)  
49 in soils and groundwater. Moreover, [11] investigated the impact of vegetation fraction on  
50 drag and pollutant transport in porous aquatic environments, developing a model that  
51 relates Reynolds number and vegetation drag to pollutant transport. [12] developed a  
52 model based on stem spacing and vegetation fraction to predict the longitudinal dispersion  
53 coefficient in low-density emergent vegetation systems.

54 To date, no research has yet employed the advection-dispersion equation in cylindrical  
55 coordinates to simulate pollutant concentration profiles in an initially contaminated porous  
56 aquatic environment.

57 The objective of this research is therefore to demonstrate the influence of vegetation  
58 volumetric fraction, Reynolds number, as well as the density and porosity of the medium,  
59 on pollutant dispersion in initially contaminated aquatic environments, using the two-  
60 dimensional advection-dispersion equation model in cylindrical coordinates.

## 61 62 **2. Materials and Methods**

### 63 **2.1 Physical and Mathematical Model**

64 In this study, we analyze the dispersion of a pollutant deposited on a cylindrical surface in an  
65 aquatic environment. Fig 1 illustrates the physical configuration of the cylindrical matrix, initially  
66 contaminated with a concentration of  $C_i$ . It shows how pollutants move through the radial  
67 coordinate  $r$  and the depth  $z$  of the matrix. The injection zone is located at the entrance of the  
68 matrix and is defined by a radius of  $r_0$ . This injection zone marks the starting point of  
69 contamination, meaning that the injected pollutants must diffuse and spread throughout the  
70 entire matrix, up to the radius  $R$  and depth  $L$ , where  $r$  and  $z$  represent the radial and vertical  
71 coordinates, respectively.

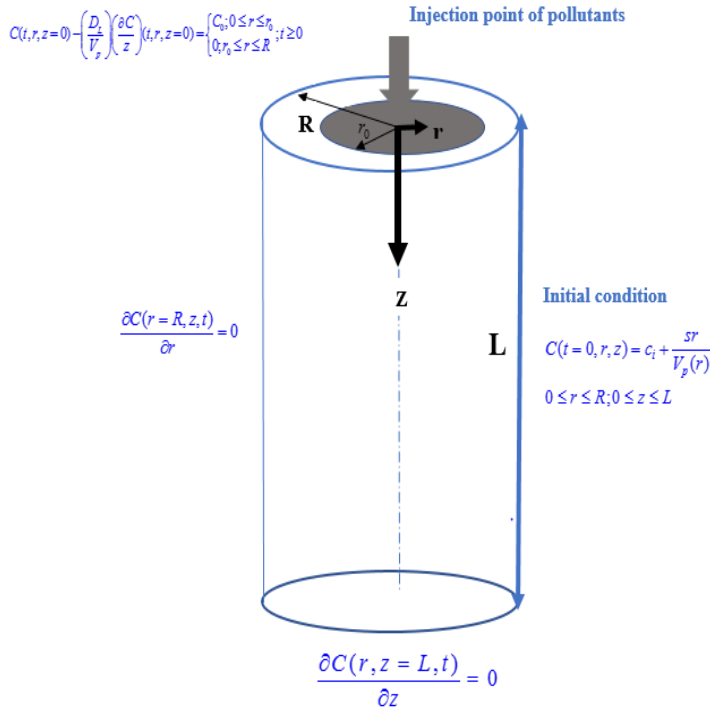


**Fig 1.** Schematic of the filter in cylindrical coordinates

The two-dimensional advection-dispersion equation model in cylindrical coordinates is used to describe the transport of contaminants or chemical and biological substances in porous media or aquatic aquifer systems. The two-dimensional advection-dispersion equation in cylindrical coordinates, with dispersion coefficients and flow velocity depending on the radial distance, is reformulated as follows [7]:

$$R_f \frac{\partial c}{\partial t} = D_L \frac{\partial^2 c}{\partial z^2} + D_T \left( \frac{\partial^2 c}{\partial r^2} + \frac{1}{r} \frac{\partial c}{\partial r} \right) - V_p \frac{\partial c}{\partial z} - k_0 C e^{\frac{\gamma}{\lambda}} \quad (1)$$

With  $\gamma$  the partition coefficient,  $\lambda$  straining coefficient,  $R_f = \frac{\rho k_0}{\theta}$  the retardation coefficient,  $\theta$  the porosity of the medium,  $\rho$  the density of the medium,  $k_0$  the adsorption coefficient,  $V_p$  the flow velocity,  $D_L = 0.3 \left[ (\phi C_D)^{\frac{1}{3}} V_p \right] l_t$  the longitudinal dispersion coefficient,  $D_T = D_L / 10$  the transverse dispersion coefficient,  $C_D$  the drag coefficient, and  $l_t$  the turbulence length [13].

## 2.2. Description of Physical Parameters

### 2.2.1. Flow Velocity

The transport velocity of pollutants in porous aquatic environments, particularly those containing vegetation, is influenced by several parameters such as vegetation fraction  $\phi$ ,

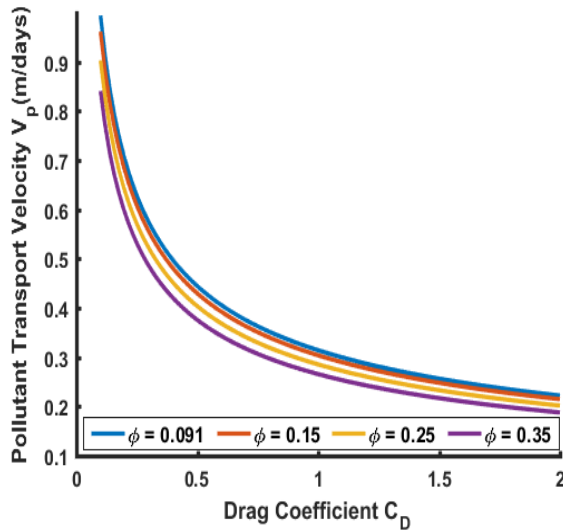
117 drag coefficient  $C_D$ , water surface area  $S$ , and gravitational acceleration  $g$  [11,13]. Vegetation  
 118 acts as a drag source that slows down water flow and consequently reduces the contaminant  
 119 transport velocity. The drag generated by vegetation is often modeled using a quadratic law  
 120 that relates the drag force to the medium's density  $\rho$ , the mean flow velocity  $V_p$ , and the  
 121 vegetation's average drag coefficient  $C_D$ , expressed as follows:

$$122 \quad F_D = \frac{1}{2} \rho C_D a V_p^2 \quad (2)$$

123 The slowdown of the flow not only alters the average velocity but also changes the vertical  
 124 distribution of velocity within the water column. Emergent vegetation leads to a significant  
 125 reduction in horizontal velocity, particularly in areas with high vegetation density. By  
 126 considering the effect of vegetation on flow dynamics, the spatially averaged velocity in a  
 127 vegetated channel can be expressed as a function of the water surface slope  $S$ , the drag  
 128 coefficient, and the pressure gradient induced by the water slope, using the following equation  
 129 from [13]:

$$130 \quad V_p = \sqrt{\frac{2gs(1-\phi)}{C_D a}} \quad (3)$$

131 This relationship shows that the presence of vegetation, characterized by a high volumetric  
 132 fraction and a significant drag coefficient, reduces the flow velocity  $V_p$  (see Fig. 2). Moreover,  
 133 studies by [13] indicate that the spatial arrangement of vegetation, as well as the diameter and  
 134 density of the stems, significantly influence the drag coefficient and, consequently, the  
 135 pollutant transport velocity.



136

137 **Fig 2 Variation of Pollutant Flow Velocity as a Function of the Drag Coefficient**

138

139

### 140 2.2.2 Drag Coefficient

Drag coefficients  $C_D$  play a key role in the dynamics of flows in aquatic porous media, particularly when simulating the resistance introduced by vegetation structures and other materials within the fluid [11,12,14]. The expression simplifying the dependence of drag on the volumetric Reynolds number is proposed, on the one hand, by:

$$C_D = 2 \left( \frac{a_0}{R_{ev}} + a_1 \right) \quad (4)$$

With  $a_0$  and  $a_1$  as empirical coefficients capturing the impact of flow resistance based on the characteristics of the fluid and obstacles, and  $R_{ev}$  the Reynolds number, which characterizes the nature of the flow as laminar or turbulent. This expression is frequently used to model drag in systems where flow velocity and particle size are well-defined. It allows the estimation of resistance exerted by solid objects in porous media while accounting for variations in flow around the particles [13].

The second expression for the drag coefficient  $C_D$  is proposed by [15] and follows the relationship:

$$C_{D1} = \left( \frac{11 \left( \frac{R_{ev}}{1+80\phi} \right)^{-0.75} + 0.9 \left[ 1 - \exp \left( -\frac{1000(1+80\phi)}{R_{ev}} \right) \right]}{1.2 \left[ 1 - \exp \left( -\left( \frac{R_{ev}}{4500(1+80\phi)} \right)^{0.7} \right) \right]} \right) (1-\phi) \quad (5)$$

This expression takes into account the Reynolds number and the volumetric ratio of solids in the medium, as well as a series of exponential terms to model drag based on the complex interaction between the fluid and the structure of the porous medium. This model is particularly suited for environments where the spatial distribution of particles and the volumetric fraction strongly influence the flow. It allows for a more detailed description of the interference effects between particles or vegetative structures, especially in scenarios where porosity varies significantly [16]. These two expressions are crucial for understanding how vegetation or other objects in porous media influence water flow.

### 2.3 Initial and Boundary Conditions

The contaminated aquatic porous medium is initially assumed to have a background concentration  $C_i$ , represented by a linear combination of this initial concentration and a zero-order production term (7,17,18,19). The initial conditions are expressed as:

$$\begin{cases} C(t=0, r, z) = C_i + \frac{sr}{v_p} \\ 0 \leq r \leq R \\ 0 \leq z \leq L \end{cases} ; \quad (6)$$

Where  $s$  is the first-order solute production,  $r$  is the radial distance in the porous medium, At the inlet of the aquatic porous matrix, a contaminant concentration is imposed, influenced by longitudinal dispersion due to the solute flow velocity within the medium. The boundary conditions at the inlet are given by:

$$173 \quad C(t, r, z=0) - \left( \frac{D_L}{V_p} \right) \left( \frac{\partial C}{\partial z} \right) (t, r, z=0) = \begin{cases} C_0; 0 \leq r \leq r_0 \\ 0; r_0 \leq r \leq R \end{cases}; t \geq 0 \quad (7)$$

174 Where  $C_0$  is the contaminant concentration imposed at the entrance of the aquifer for  
 175  $0 \leq r \leq r_0$ ,  $r_0$  represents the region where the contaminant is introduced. This condition  
 176 represents a non-uniform contaminant input at the domain's entrance, influenced by  
 177 longitudinal dispersion.  
 178 At the exit of the aquifer and along the radial boundaries, no-flux conditions are imposed,  
 179 meaning there is no solute flux across these boundaries. The boundary conditions at the  
 180 edges are therefore:

$$181 \quad \begin{cases} \left( \frac{\partial C}{\partial r} \right) (t, r = R, z) = 0 \\ \left( \frac{\partial C}{\partial z} \right) (t, r, z = L) = 0 \end{cases} \quad (8)$$

182 Where  $r = R$  represents the outer radial boundary and  $z = L$  represents the maximum depth.  
 183 These conditions indicate that the solute flux is zero both at the radial edges and at the  
 184 longitudinal outlet of the aquifer, thus preventing any solute transfer out of the domain at these  
 185 boundaries.

## 189 2.4. Numerical Resolution

190 The numerical resolution of the two-dimensional advection-dispersion equation model in  
 191 cylindrical coordinates is based on spatial and temporal discretization. This discretization  
 192 transforms the partial differential equation into a system of algebraic equations, which can be  
 193 solved numerically using the finite difference method, a commonly used numerical technique  
 194 for solving partial differential equations (PDEs) [8,18]. The first-order temporal, radial, and  
 195 spatial discretizations are given as follows:

$$196 \quad \frac{\partial C}{\partial t} = \frac{C_{i,j}^{k+1} - C_{i,j}^k}{\Delta t} \quad (9)$$

$$197 \quad \frac{\partial C}{\partial r} = \frac{C_{i+1,j}^k - C_{i-1,j}^k}{\Delta r} \quad (10)$$

$$198 \quad \frac{\partial C}{\partial z} = \frac{C_{i,j+1}^k - C_{i,j-1}^k}{\Delta z} \quad (11)$$

199 The second-order radial and spatial discretization are given as follows

$$200 \quad \frac{\partial^2 C}{\partial r^2} = \frac{C_{i+1,j}^k - 2C_{i,j}^k + C_{i-1,j}^k}{(\Delta r)^2} \quad (12)$$

$$201 \quad \frac{\partial^2 C}{\partial z^2} = \frac{C_{i,j+1}^k - 2C_{i,j}^k + C_{i,j-1}^k}{(\Delta z)^2} \quad (13)$$

Where  $i, j$ , and  $k$  are the discretization nodes, and  $\Delta r$ ,  $\Delta x$ , and  $\Delta t$  are the radial, spatial, and temporal steps, respectively,  $0 \leq i \leq N_r, 0 \leq j \leq N_z, 0 \leq k \leq N_t$ . By combining expressions 9, 10, 11, 12, and 13 in the transport equation 1, we obtain:

$$C_{i,j}^{k+1} = \left[ 1 - 2(\beta_1 + \beta_3) - \beta_2 + \beta_4 - \Delta t k_0 e^{\frac{\gamma}{\lambda}} \right] C_{i,j}^k + \beta_1 C_{i+1,j}^k + \beta_3 C_{i,j+1}^k + (\beta_1 + \beta_2) C_{i-1,j}^k + (\beta_3 - \beta_4) C_{i,j-1}^k \quad (14)$$

Where  $\beta_1 = \frac{\Delta t(D_L)}{R_f \Delta x^2}, \beta_2 = \frac{\Delta t(V_p)}{R_f \Delta z}, \beta_3 = \frac{\Delta t(D_T)}{R_f \Delta r^2}, \beta_4 = \frac{\Delta t(D_T)_i}{i R_f \Delta r^2}$ . The discretization of the initial boundary conditions is given successively by the following relations:

$$\begin{cases} C_{i,j}^0 = C_i + \frac{is}{V_p} \\ 0 \leq i \leq N_r, 0 \leq j \leq N_z \end{cases} \quad (15)$$

$$\begin{cases} \Delta z \left( 1 + \left( \frac{D_L}{V_p} \right)_i \right) C_{i,j=0}^k = \Delta z C_0 + \left( \frac{D_L}{V_p} \right)_i C_{i,j=0}^k, 0 \leq i \leq \frac{N_r}{4} \\ \Delta z \left( 1 + \left( \frac{D_L}{V_p} \right)_i \right) C_{i,j=0}^k = \left( \frac{D_L}{V_p} \right)_i C_{i,j=0}^k, \frac{N_r}{4} \leq i \leq N_r \end{cases} \quad (16)$$

The discretization of the boundary conditions is given by the following relationships:

$$\begin{cases} C_{N_r,j}^k = C_{N_r-1,j}^k \\ C_{i,N_z}^k = C_{i,N_z-1}^k \end{cases} \quad (30)$$

We analyzed the numerical solutions using the following model parameters:  $C_0=1, \rho_d=1.68$  g/L,  $k_0=0.9$  g/L,  $\theta=0.33$ ,  $a_0=0.085, a_1=11$ ,  $\phi=0.091, 0.35$ ,  $R_{ev}=25, s=0.007, C_i=0.01$ ,  $g=9.8$  m/s<sup>2</sup>,  $l_t=0.1$ ,  $\gamma=0.0007$ ,  $\lambda=0.474$ , these parameters are based on the work of [7,8,9,12,13,18,19] who studied the role of plant structures in modifying hydrodynamic flows and transport processes in aquatic porous media.

### 3. Results and discussion:

#### 3.1. Influence of vegetation volumetric fraction and Reynolds number on pollutant dispersion and their ecological effects in aquatic environments.

This section evaluates the influence of environmental parameters on pollutant dispersion in aquatic environments, taking into account the interactions between vegetation, Reynolds

number, and hydrodynamic properties. The effects of these pollutants on the ecosystem, particularly on flora, fauna, and overall water quality, are also considered.

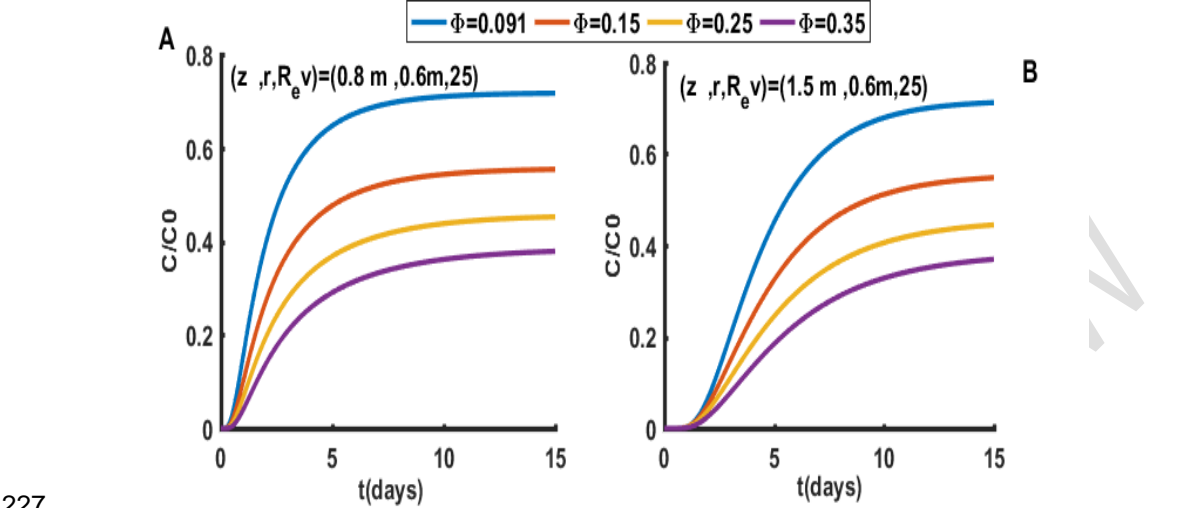


**Fig. 3: Influence of vegetation volumetric fraction on pollutant concentration over time at different depths ( $z = 0.8\text{ m}$  and  $z = 1.5\text{ m}$ ).**

Fig. 3 demonstrates that the vegetation volumetric fraction  $\phi$  ( $\phi = 0.091, 0.13, 0.26$ ) significantly influences pollutant concentration over time. These high concentrations can lead to a degradation of water quality, with direct consequences on aquatic flora and fauna, as shown in the works of [13,14]. For the observation points  $(z, r) = (0.8\text{ m}, 0.6\text{ m})$  in Fig. 3a and  $(z, r) = (1.5\text{ m}, 0.6\text{ m})$  in Fig. 3b, pollutant concentration increases exponentially, which could cause significant ecological disturbances, such as a reduction in photosynthesis for aquatic plants and toxic effects on fish and invertebrates. It appears that pollutant retention is greater at a depth of  $z = 1.5\text{ m}$ , where pollutants disperse less rapidly. This corroborates the findings of [16], who shows better particle capture in deeper environments but focuses only on rigid plant structures. Our results provide a more detailed understanding of the interactions between flexible vegetation and flow dynamics, offering a more comprehensive perspective on the dynamic effects of submerged vegetation on pollutant dispersion. An additional observation is that pollutant concentration decreases with an increase in the vegetation volumetric fraction, regardless of depth. This can be attributed to the increase in natural obstacles caused by vegetation, acting as a physical barrier and thus promoting pollutant capture. The results from Fig. 4 reveal an increase in pollutant retention as the Reynolds number increase ( $(Re = 52 \cdot 10^5, 54 \cdot 10^5)$ ), as noted by [13,20].



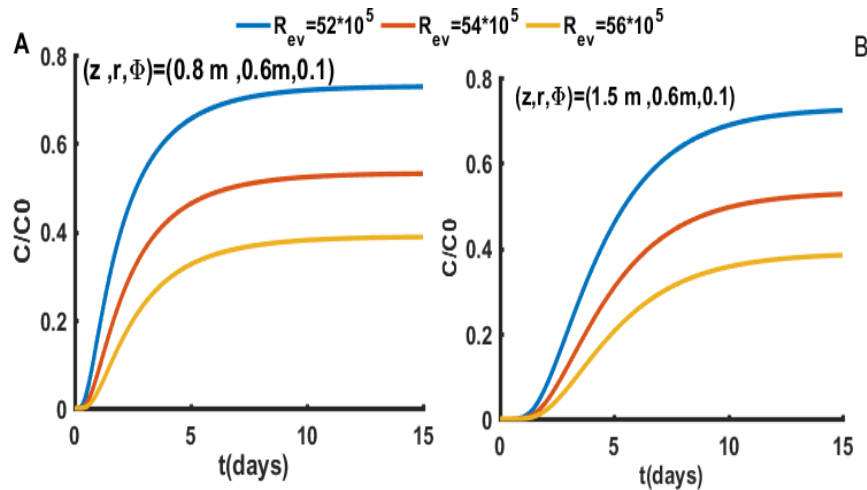


**Fig 4. Effect of Reynolds number on pollutant dispersion over time at different depths ( $z = 0.8$  m and  $z = 1.5$  m).**

These studies indicate that turbulence generated by shear forces around rigid or flexible aquatic plants directly influences the pollutant retention capacity in the pores of aquatic matrices. In our case, a decrease in Reynolds number reduces turbulence intensity, allowing for better pollutant retention, particularly at a depth of  $z = 1.5$  m. This phenomenon could lead to higher contamination accumulation in deeper areas, with long-term ecological impacts, such as the alteration of aquatic wildlife communities. These results go beyond the work of [13] by showing an explicit link between a decrease in Reynolds number and reduced pollutant dispersion in aquatic porous matrices. This highlights the importance of considering the potential ecological effects of hydrodynamic parameters on wildlife and plant life in the management of polluted aquatic environments.

### **3 .2. Influence of vegetation volumetric fraction on the radial dispersion ( $r$ ) and depth ( $z$ ) of pollutants in aquatic environments using the first model.**

In this section, two values of the volumetric fraction ( $\varphi = 0.091$  in fig3.A and  $\varphi = 0.35$  in fig3.B) were used to evaluate the distribution of pollutants after 2 days.

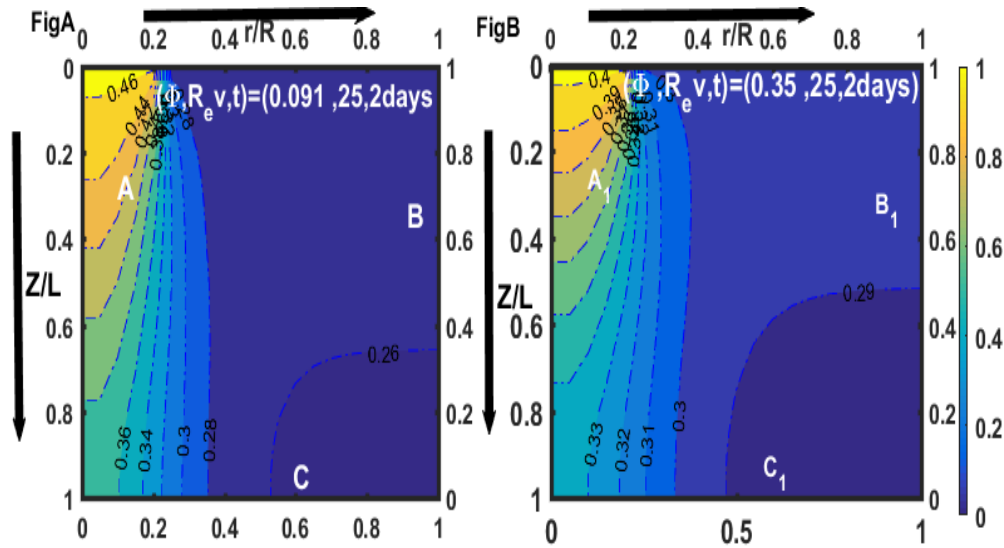


**Fig. 5 Spatial distribution of pollutants in an aquatic system  $(\phi, R_e, t) = (0.091, 25, 2 \text{ days})$ .**

It is observed in Fig. 5 that for  $\phi = 0.091$ , pollutant concentrations are higher, with a concentration difference between points A ( $r/R = 0.1, z/L = 0.25$ ) and B ( $r/R = 0.9, z/L = 0.25$ ) of 0.1685, or 16.85%. In contrast, for  $\phi = 0.35$ , the concentration difference between these same points is 0.0822, or 8.22%. This decrease in pollutant dispersion as the vegetation volumetric fraction increases suggests that the presence of vegetation slows down the flow of pollutants through the aquatic porous medium. This results in reduced spread and accumulation in specific areas. The impact of pollutants on aquatic ecosystems is largely influenced by this dynamic. Indeed, reduced pollutant dispersion can lead to higher concentrations in certain areas, which may have devastating effects on aquatic flora and fauna. Organisms living in these environments may be exposed to elevated levels of pollutants, leading to consequences such as reproductive disruptions, increased mortality, or changes in population structure. Aquatic plant species, in turn, may undergo physiological alterations due to the accumulation of toxic substances, affecting the overall health of the ecosystem. Furthermore, depth ( $z$ ) appears to play a more significant role than radial distance ( $r$ ) in pollutant dispersion, implying a vertical stratification of concentrations in the aquatic environment. This stratification can have complex effects on different ecological layers, as some organisms are more sensitive to contaminants at certain depths. Higher concentrations of pollutants at specific depths can lead to dead zones where aquatic life is severely compromised. These observations align with the work of [12], who showed that higher vegetation fractions reduce pollutant accumulation. However, their results were limited to environments with vegetation densities below 0.1, while this study explores scenarios with fractions up to 0.35. This shows that in systems with denser vegetation, the effect on pollutant dispersion is even more pronounced. The increase in vegetation volumetric fraction limits pollutant dispersion in aquatic environments, reducing their overall spread but potentially exacerbating their impact in certain areas. This dynamic highlights the importance of understanding the interaction between vegetation, depth, and pollutant dispersion to assess the long-term effects of contaminants on aquatic ecosystems.

### 3.3 Influence of Density, Porosity, and Vegetation Volumetric Fraction on Pollutant Dispersion in Porous Aquatic Environments

Fig. 6 illustrates the influence of the aquatic medium's density ( $\rho = 1, 1.4, 1.8$ ) on the evolution of pollutant concentration as a function of vegetation volumetric fraction. This analysis is carried out using the numerical solution associated with the two drag coefficient models described by relations 4 and 5.

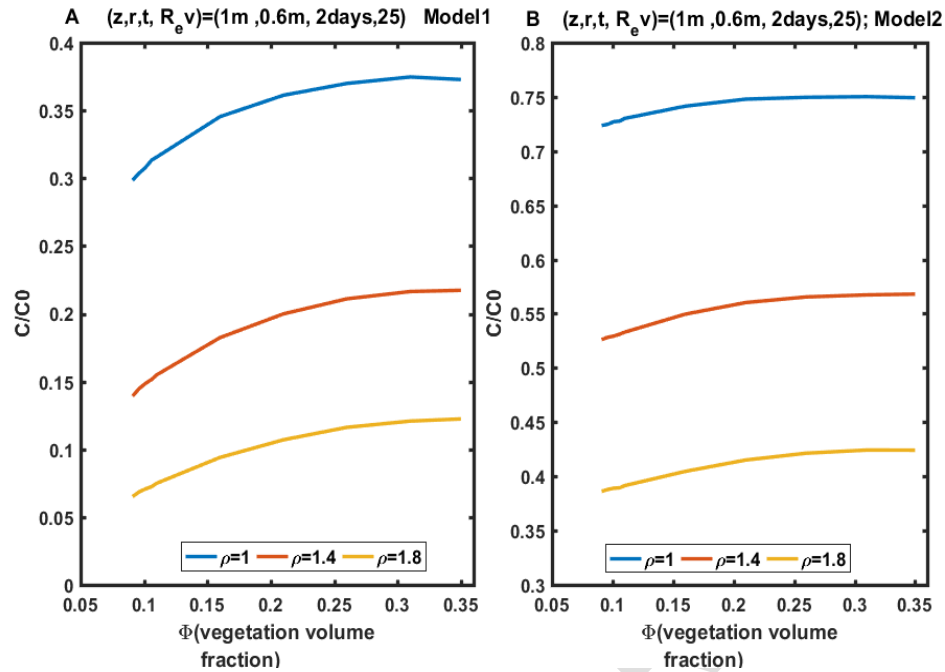


**Fig. 6 Impact of Medium Density on Pollutant Dispersion as a Function of Vegetation Volumetric Fraction in a Porous Aquatic Medium**

Pollutant concentrations are measured at a given depth and radius ( $z = 1$  m,  $r = 0.6$  m), and the results show an increase in concentrations with the vegetation volumetric fraction, regardless of the model used. However, the observed concentrations are higher in Model 2 than in Model 1. This difference is attributed to the generalization of the drag coefficient in Model 2, which takes into account the Reynolds number, applicable to both isolated vegetation and dense arrays, as discussed by [15].

This increase in concentrations with the vegetation volumetric fraction is notable because an increase in volumetric fraction generally leads to a decrease in flow velocity. A lower velocity favors pollutant retention, thus reducing pollutant dispersion. The results also show that the highest concentrations are observed in denser media ( $\rho = 1.8$ ). This suggests that the medium's density plays an important role in pollutant retention, which could lead to greater accumulation in certain areas, increasing risks for local fauna and flora. The lowest concentrations are observed for the density  $\rho = 1$ , showing that pollutant dispersion in aquatic environments is closely linked to the medium's density.

These results are more complex than those reported by [12], whose work mainly focuses on longitudinal dispersion through wake dispersion mechanisms, relevant for low vegetation densities. These mechanisms are generally insufficient to explain dispersion in more complex environments with dense vegetation, where other processes, such as turbulent diffusion or vortex trapping, may become significant. On the other hand, [13] described the medium density, including vegetation or suspended particle density, as an important factor in pollutant dispersion, although his study does not specifically address dispersion in porous aquatic media. His work focuses instead on surface flow dynamics induced by vegetation without exploring in detail the density of the pore matrix itself or its interactions with flows.

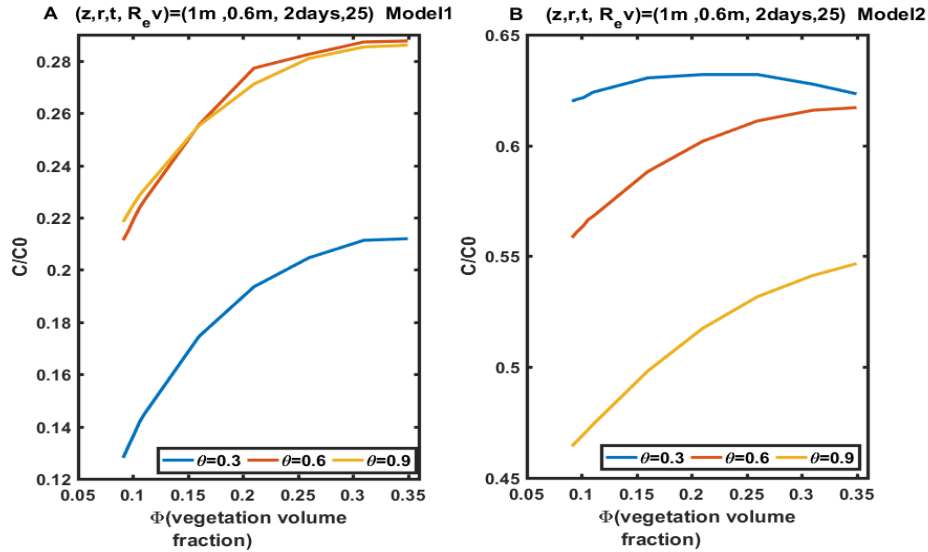


**Fig.7 Effect of Medium Porosity on Pollutant Distribution in Relation to Vegetation Volumetric Fraction in a Porous Aquatic Environment**

Fig. 7 highlights the influence of medium porosity ( $\phi = 0.3, 0.6, 0.9$ ) on pollutant distribution as a function of vegetation volumetric fraction. The results show a uniform increase in pollutant concentrations with vegetation volumetric fraction, regardless of the model used. However, the most pronounced pollutant retention, i.e., the lowest concentrations, is observed in Model 1, unlike in Model 2. [15] primarily studied Model 2 without exploring other models, which limits their analysis. The highest concentrations are observed in environments with high porosity ( $\phi = 0.9$ ), while the lowest concentrations are associated with lower porosity ( $\phi = 0.3$ ) for both models. These results confirm that pollutant concentration increases with medium porosity, which has significant implications for the dynamics of aquatic ecosystems. High porosity allows for faster pollutant diffusion, increasing their spread into deeper or more distant areas, potentially exacerbating the impact on aquatic species and vulnerable ecosystems. The presented results are more comprehensive than those of [11], who measured drag on sets of rigid elements without explicitly considering medium porosity. In aquatic porous matrices, porosity plays a crucial role in pollutant transport and retention. These results demonstrate that porosity directly influences the availability of pollutants to aquatic flora and fauna, potentially increasing the risks of bioaccumulation and long-term toxic effects. Including this parameter in dispersion models is therefore essential for understanding the complex interactions between pollutants and the aquatic ecosystem, particularly in porous environments.

### 3.3. Model Validation

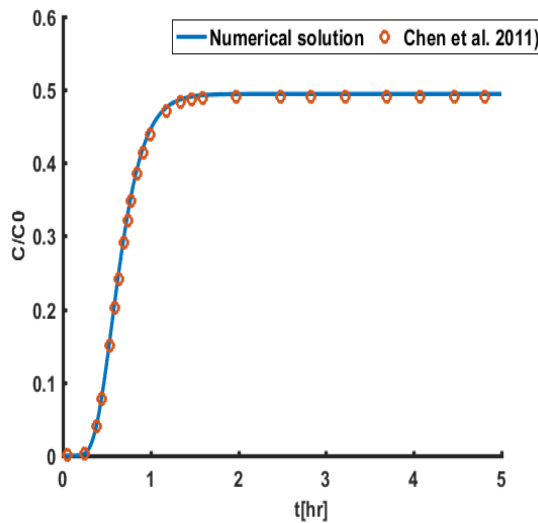


**Fig. 8 Validation of numerical solution with analytical solution obtained by [7].**

Fig. 8 above represents the validation of the numerical solution for the two-dimensional advection-dispersion equation in cylindrical coordinates with the analytical solution obtained by [7], used in this study to evaluate solute transport in aquatic porous media. This figure demonstrates a close agreement between the analytical and numerical results. These observations strengthen the validity and reliability of the model used to study solute transport in aquatic porous media.

#### 4. CONCLUSION

In this article, we proposed a numerical solution to the advection-dispersion equation in cylindrical coordinates using the finite difference method. This approach allows for the evaluation of the impact of several parameters, including vegetation volumetric fraction, Reynolds number, density, and porosity of the medium, on the behavior of pollutants in initially contaminated aquatic porous environments. The analysis of the results obtained shows that the concentration of pollutants decreases significantly with the increase in vegetation volumetric fraction. Furthermore, as a water point located in an aquatic porous medium age, the dispersion phenomenon, influenced by the vegetation fraction and Reynolds number, tends to evenly distribute the pollution plume or front throughout the system. The pollutant concentrations predicted by model 2, which incorporates drag effects, are higher than those predicted by model 1. This highlights the importance of considering the complexity of interactions between these parameters for better modeling of the processes. Additionally, the porosity and density of the medium are found to have a crucial impact on the retention and propagation of pollutants, thus influencing the dynamics of aquatic ecosystems. These results emphasize the importance of considering these interactions for a more accurate assessment of the ecological impacts of pollutants in aquatic environments.

391  
392  
393  
394

## 395 **Disclaimer (Artificial Intelligence)**

396 The author(s) hereby declare that NO generative AI technologies, such as  
397 Large Language Models (ChatGPT, COPILOT, etc.) or text-to-image  
398 generators, have been used during the writing or editing of this manuscript.

399  
400  
401

## **REFERENCES**

- 402 [1] Lie, M., Binhudayb, F. S., Thao, N. T. T., & Kristanti, R. A. (2024). Assessing the Impact of  
403 Pharmaceutical Contamination in Malaysian Groundwater: Risks, Modelling, and Remediation  
404 Strategies. *Tropical Aquatic and Soil Pollution*, 4(1), 43-59.
- 405 [2] Lo, M. L., Wade, M., Ndao, S., Diallo, A., & Sissoko, G. (2016). Numerical modeling of  
406 solute transport: Predicting the risk of groundwater contamination in the Niayes area (Senegal)  
407 by pesticides. *International Journal of Innovation and Applied Studies*, 17(4), 1358.
- 408 [3] Jampani, M., Mateo-Sagasta, J., Chandrasekar, A., Fatta-Kassinos, D., Graham, D. W.,  
409 Gothwal, R., ... & Langan, S. (2024). Fate and transport modelling for evaluating antibiotic  
410 resistance in aquatic environments: Current knowledge and research priorities. *Journal of*  
411 *Hazardous Materials*, 461, 132527.
- 412 [4] Gramling, C. M., Harvey, C. F., & Meigs, L. C. (2002). Reactive transport in porous media:  
413 A comparison of model prediction with laboratory visualization. *Environmental Science &*  
414 *Technology*, 36(11), 2508-2514.
- 415 [5] Zhang, R., Huang, K., & Xiang, J. (1994). Solute movement through homogeneous and  
416 heterogeneous soil columns. *Advances in Water Resources*, 17(5), 317-324.
- 417 [6] Ashraf, M., Guleria, A., Ahammad, S. Z., & Chakma, S. (2024). Implementation of temporal  
418 moments to elucidate the reactive transport of metformin and erythromycin in the saturated  
419 porous media. *Environmental Science and Pollution Research*, 31(35), 47801-47817.
- 420 [7] Chen, J. S., Chen, J. T., Liu, C. W., Liang, C. P., & Lin, C. W. (2011). Analytical solutions  
421 to two-dimensional advection–dispersion equation in cylindrical coordinates in finite domain  
422 subject to first-and third-type inlet boundary conditions. *Journal of Hydrology*, 405(3-4), 522-  
423 531.
- 424 [8] Nganso, A. S. N., Togue, F. K., & Mbane, C. B. (2024). Effects of the injection radius and  
425 varying velocity on solute transport in a finite porous medium with radial geometry. *Sādhana*,  
426 49(2), 118.

- 427 [9] Hwang, G. (2021). Analytical solution for the two-dimensional linear advection-dispersion  
428 equation in porous media via the fokas method. *Journal of Applied Analysis & Computation*,  
429 11(5), 2334-2354.
- 430 [10] Ramirez, R., Martí, V., & Darbra, R. M. (2023). Aquatic ecosystem risk assessment  
431 generated by accidental silver nanoparticle spills in groundwater. *Toxics*, 11(8), 671.
- 432 [11] Tseng, C. Y. (2022). *From substrate to surface: An integrated study on the Interfacial*  
433 *transfer and sediment suspension based on a turbulence perspective in vegetated*  
434 *flows* (Doctoral dissertation, University of Illinois at Urbana-Champaign).
- 435 [12] Sonnenwald, F., Stovin, V., & Guymer, I. (2019). A stem spacing-based non-dimensional  
436 model for predicting longitudinal dispersion in low-density emergent vegetation. *Acta*  
437 *Geophysica*, 67(3), 943-949.
- 438 [13] Yang, J. Q. (2024). Solute flow and particle transport in aquatic ecosystems: A review on  
439 the effect of emergent and rigid vegetation. *Environmental Science and Ecotechnology*,  
440 100429.
- 441 [14] King, A. T., Tinoco, R. O., & Cowen, E. A. (2012). A k- $\epsilon$  turbulence model based on the  
442 scales of vertical shear and stem wakes valid for emergent and submerged vegetated flows.  
443 *Journal of Fluid Mechanics*, 701, 1-39.
- 444 [15] Cheng, N. S. (2013). Calculation of drag coefficient for arrays of emergent circular  
445 cylinders with pseudofluid model. *Journal of Hydraulic Engineering*, 139(6), 602-611.
- 446 [16] Gurmu, G. (2019). Soil organic matter and its role in soil health and crop productivity  
447 improvement. *Forest Ecology and Management*, 7(7), 475-483.
- 448 [17] Singh, A., Sharma, R., Pant, D., & Malaviya, P. (2021). Engineered algal biochar for  
449 contaminant remediation and electrochemical applications. *Science of the Total*  
450 *Environment*, 774, 145676.
- 451 [18] Madie, C. Y., Togue, F. K., & Wofo, P. (2022). Numerical solution of the Burgers equation  
452 associated with the phenomena of longitudinal dispersion depending on time. *Heliyon*, 8(7).
- 453 [19] Das, R., Vecitis, C. D., Schulze, A., Cao, B., Ismail, A. F., Lu, X., ... & Ramakrishna, S.  
454 (2017). Recent advances in nanomaterials for water protection and monitoring. *Chemical*  
455 *Society Reviews*, 46(22), 6946-7020.
- 456 [20] Nian, T. K., Guo, X. S., Fan, N., Jiao, H. B., & Li, D. Y. (2018). Impact forces of submarine  
457 landslides on suspended pipelines considering the low-temperature environment. *Applied*  
458 *Ocean Research*, 81, 116-125.

459